Evaluation of Quality Parameters of Açaí Oil During Thermal Oxidation Using NIRS and Chemometrics

B. V. C. Rodrigues[1] · D. R. Pompeu[2] · C. A. N. P. Herman[1]

Abstract

Near-infrared spectroscopy and chemometrics were investigated as a rapid analytical method to evaluate quality parameters of açaí oil during thermal oxidation under accelerated conditions. A two-factors full factorial design with 2 levels for the treatment (without antioxidant and with 400 ppm of myricetin) and 8 levels for the oxidation time (giving insight of the initial stage of oil oxidation) was used. Three quality parameters (peroxide, conjugated diene, and *p*-anisidine values) were monitored by reference analysis. Multi-factorial analysis of variance and estimation of the order of the kinetic models pointed out that both factors and their interaction had a significant effect on the quality parameters (p value < 0.05). In particular, the supplementation of açaí oil allowed delaying the induction period from 2 to 5 days. Chemometrics reveals that the best spectral region for development of models was 10,000 to 6500 cm^{-1}. Calibration models by partial least square regression method (using full internal cross-validation and external validation) for the prediction of peroxide and *p*-anisidine values present high determination coefficient (> 0.83) and ratio of prediction to deviation (> 2.9) that indicated good performance for the prediction of new independent samples. High sensitivity ($> 83\%$) and accuracy ($> 95\%$) of the linear discriminant analysis, obtained when the first derivative was used as pre-treatment, were indicators of a suitable technique for classifying new independent samples. Principal component analysis showed the formation of two clusters corresponding to açaí oil samples safe and unfit for commercialization. In conclusion, near-infrared spectroscopy revealed to be a powerful alternative analytical technique for prediction and classification of açaí oil samples at industrial scale.

Keywords *Euterpe oleracea* · Lipid · Peroxidation · Prediction · Classification

Introduction

The consumption of foods rich in unsaturated oils has been encouraged in recent years as their important role in human nutrition and health has been demonstrated scientifically. Numerous studies have suggested that a frequent intake of unsaturated fatty acids provides prevention and control of various diseases. Açaí oil, which is of interest in this work, consists of more than 70% of unsaturated fatty acids

(Pacheco-Palencia et al. 2008; Batista et al. 2016) and is rich in natural antioxidants, such as apolar phenolic compounds (Pacheco-Palencia et al. 2008), tocopherols (Darnet et al. 2011), tocotrienols (Lubrano et al. 1994), and phytosterols (Schauss 2010). Açaí oil is known to present antidiarrheic (Plotkin and Balick 1984), hypocholesterolemic (Souza et al. 2012), antimicrobial (Filho and Pereira 2012), anticarcinogenic (Pacheco-Palencia et al. 2008; Monge-Fuentes et al. 2017), anti-inflammatory, and antinociceptive (Favacho et al. 2011) activities. Due to these chemical and biological properties, açaí oil turns out very interesting for food, cosmetic, and pharmaceutics industries.

However, oils presenting high proportions of unsaturated fatty acids are very sensible to oxidation, which can be induced in the presence of oxygen, light, heat, and/or enzymes. Such process has traditionally received considerable attention because it causes economic loss to the industry, shortens food shelf life, and produces unpleasant flavors and odors as well as compounds that may be prejudicial to

✉ C. A. N. P. Herman
  christelle@ufpa.br; christelle.herman.pompeu@gmail.com

[1] Centre for Valorization of Amazonian Bioactive Compounds, Universidade Federal Do Pará, Av. Perimetral da Ciência, km 01, s/n, Belém, PA 66095-780, Brazil

[2] Departamento de Tecnologia de Alimentos, Centro de Ciências Naturais E Tecnologia, Universidade Do Estado Do Pará, Trav. Enéas Pinheiro nº2626, Belém, PA 66095-100, Brazil

human health (Choe and Min 2006). Oil oxidation can be delayed by the addition of low concentrations of some exogenous lipophilic antioxidants (as example of tocopherols, carotenoids, or phenolic compounds) (Laguerre et al. 2007; Choe and Min 2009). The main effect of such practice is the increase of the induction period (Kiritsakis and Shahidi 2017). The exogenous antioxidant tested in the context of this work is myricetin.

Many analytical techniques can be used for monitoring oil oxidation; each one provides complementary information of both primary and secondary oxidation products (Barriuso et al. 2013). Reference and empirical analysis are widely used as they allow a confident determination of some quality parameters of the status of oil oxidation. Nowadays, they tend to be replaced by alternative and more modern techniques that present advantages to be easy, low-cost, fast, non-destructive, and real-time methods. One of such technique is the near-infrared spectroscopy (NIRS), which is investigated in our work.

A recent search in scientific databases pointed out that NIRS continues to be poorly used as an analytical tool for edible oil. When used, it mainly concerns the development of regression or prediction models for parameters of composition (as example, moisture or protein contents, fatty acid profile), authenticity, adulteration, or quality of common oils (as example, olive, soybean, palm, rapeseeds, and sunflower). Very few studies have focused on the development of NIRS methods for assessing quality parameters during oil oxidation. Moreover, most of authors used an ample range of oils samples (see for example Costa et al. 2016; Sánchez et al. 2013; Canha et al. 2012; Armenta et al. 2007; Cozzolino et al. 2005) rather than performing a real oil oxidation. Eventually, very few realized a frequent monitoring of the samples during oil oxidation (see for example Daoud et al. 2020; Hong et al. 2017; Muresan et al. 2016; Wójcicki et al. 2015; Yildiz et al. 2001; Moh et al. 1999; Cho et al. 1998). Most of them demonstrate that NIRS, coupled with chemometrics, has the capacity to predict some quality parameters during oil oxidation, such as acidity, free fatty acid, p-anisidine value, total polar materials, peroxide value, conjugated diene value, or oxidative stability index. These papers also concluded that more studies are needed to test this approach on various other oils.

In this context, the main objective of our study was to investigate for the first time the use of NIRS and chemometrics as an analytical tool for monitoring quality parameters of açaí oil with and without supplementation during thermal oxidation. More specifically, our paper aimed to evaluate if the supplementation of açaí oil with myricetin has a significant effect on the protection against oxidation. This was achieved by the use of an experimental design allowing giving insight of the initial stage of oil oxidation, which is very little explored in the literature, the determination of the order

of the kinetic models, and the estimation of the induction period. Moreover, our study aimed to determine if NIRS has the ability to predict correctly quality parameters of açaí oil during oxidation. This was achieved by the development of calibration models by partial least square regression method, and the discussion of the best NIR spectral region aiming to maximize the model performance. Eventually, our work aimed to verify if NIRS has the ability to discriminate oil samples during oxidation, and in particular to detect quickly when açaí oil samples became unfit for commercialization. This was achieved by the use of the linear discriminant analysis and principal component analysis.

Materials and Methods

Raw Material

Three independent bottles of 1L of açaí oil were purchased from Mundo dos Óleos (Cruzeiro, Brasília, Brazil). It consists of a 100% pure and natural oil extracted by cold pressing, maceration, and filtration, without the addition of mineral oil, petrolatum, preservatives, essences, or any other ingredients that may violate the extracted raw material. The myricetin was purchased from Extrasynthese (Genay, France) (Reference 1127 S, Batch 17, CAS 529–44-2).

Oil Oxidation Conditions

The thermal oxidation of açaí oil was performed under accelerated conditions, according to the Schaal oven stability test (AOCS Cg 5–97, 2017), with small adaptations. The assays were performed in properly identified 100-mL amber bottles containing approximately 20 mL of açaí oil. The unopened bottles containing the samples were submitted to accelerated conditions of oxidation at 60 °C for 7 days in a stove with air recirculation (drying and sterilizing stove, SOLAB SL-100, Piracicaba, São Paulo, Brazil). The initial experimental point, namely "day 0," underwent the oil oxidation for 30 min. This minimum time of 30 min, required for the oil temperature reaching 60 °C, was determined by preliminary tests. As soon as the bottles were taken from the stove according to the experimental design, they were saturated with nitrogen atmosphere (N_2) and stored at -20 °C until the analysis.

Experimental Design

The experiments were performed according to a full factorial design with two factors: treatment and oxidation time. Two levels were evaluated for the treatment: açaí oil without antioxidant ("C-") and açaí oil supplemented with 400 ppm of myricetin ("My"). Eight levels were evaluated for the

oxidation time, which correspond to the residence time of the samples in the stove: 0, 0.5, 1.0, 1.5, 2.0, 3.0, 5.0, and 7.0 days. Each experimental point was repeated three times using three individual bottles of açaí oil. The 48 bottles were properly identified, and placed randomly in the stove.

Reference Analysis

Quality Parameters

Primary (peroxide value and conjugated diene value) and secondary (*p*-anisidine value) oxidation products in the samples of açaí oil were evaluated according to official methodologies. The peroxide value (PV), that quantifies the amount of hydroperoxides, was evaluated according to the AOCS SURPLUS Official Method Cd 8–53 (2009)—Acetic Acid-Chloroform Method, using 5 g of açaí oil sample. PV was expressed as milliequivalents of peroxide per kilogram of sample (mEq O_2/kg). The conjugated diene value (CD), which is relative to the fatty acid with two or more conjugated double bonds, was determined according to the AOCS Official Method Cd 7–58 (2017), using 0.065 g of açaí oil sample. CD was expressed as percent content (% w/w) as suggested by IUPAC Method 2.206. The *p*-anisidine value (pAV), which is an indicative of the amount of unsaturated aldehydes, was quantified according to the AOCS Official Method Cd 18–90 (2017), using 0.5 g of açaí oil sample. pAV is a dimensionless value (pAV unit).

Statistical Analysis

The results were expressed as the mean value ± the standard deviation ($n = 3$). The results were submitted to the multifactorial analysis of variance (MANOVA) and the Fisher LSD test, with a significance level of 95% ($\alpha = 0.05$), using the STATISTICA software version 7.0 (Statsoft Inc., Tulsa, OK, USA). In the graphical representations of the results, same case letters imply that the values are not significantly different according to the statistical analysis realized.

Rate of Production of Oxidation Products

Equation (1) expresses the rate of production of the oxidation products (per unit of time) during oil oxidation. Considering that the quality parameter evaluated is noted A, $r_{A,dt}$ is the rate of variation of *A* per unit of time; *dA* is the difference of the values of *A* in the time interval, *dt*, considered; *k* is the rate constant kinetic; and *n* is the apparent order of the reaction. The kinetics of oil oxidation are frequently described by zero ($n = 0$), first ($n = 1$), or eventually second ($n = 2$) order kinetic models.

$$r_{A,dt} = \frac{dA}{dt} = k[A]^n \tag{1}$$

Near-Infrared Spectroscopy

Spectral Acquisition

The NIR spectra of açaí oil samples were obtained using an Antamis II FT-NIR Analyzer equipment from ThermoFischer Scientific (Alto de Pinheiros, São Paulo, Brazil), coupled to a fiber optic SabIR transflectance probe. Açaí oil contained in the amber bottles was transferred to 50-mL beakers externally protected with aluminum fold. The spectra were obtained at 25 °C by accumulation of 32 scans in the spectral regionfom 10,000 to 4000 cm^{-1} with a resolution of 10 cm^{-1}. The measurement was performed in triplicate. The NIR spectra of each sample were the average of the three spectra collected.

Data Processing

NIR spectral data were analyzed using the software The Unscrambler X 10.3 (CAMO Software Inc.). Different preprocessing strategies of the raw spectral data were evaluated. First, different NIR spectral regions were studied: whole spectra 10,000–4000 cm^{-1}, cut 1 10,000–6500 cm^{-1}, cut 2 6100–5100 cm^{-1}, cut 3 4800–4000 cm^{-1}, and the combination between cut 2 and cut 3 (see Fig. 2). Then, different pre-treatments were applied to the NIR spectral data: baseline, detrend, first, and second derivatives, multiplicative scatter correction (MSC), smoothing, normal variate (SNV). Such pre-treatments were applied individually or in combination. The first and second derivatives and smoothing pre-treatments were performed using the algorithm of Savitzky–Golay (5 points and second-order filtering).

Calibration Models by Partial Least Square Regression Method

The partial least square (PLS) regression method was used to identify quantitative correlation between NIR spectral data and the three quality parameters (i.e., peroxide value, conjugated diene value, and *p*-anisidine value) obtained by reference analysis. A PLS regression model was developed for each NIR spectral regions using the raw NIR spectra (i.e., without pre-treatment). Two strategies were used. First, due to the limited number of samples, the calibration was assessed by using the full leave-one-out internal cross-validation procedure (Wójcicki et al. 2015). Then, the experimental data were divided in two sets for realizing an external validation procedure. The statistical parameters used to evaluate the model performances included the root mean of

error of calibration (RMSEC), cross-validation (RMSECV), and validation (RMSEV) and the determination coefficient (R^2). The ratio of prediction to deviation (RPD) value, corresponding to the ratio of the SD (deviation) of cross-validation or validation set to the RMSECV or RMSEV, was also calculated. The optimum number of PLS factors was determined applying the root mean error (RMSE) and error (SE).

Principal Component Analysis and Linear Discriminant Analysis

An exploratory NIR spectral data analysis by PCA was applied to the raw NIR spectra (i.e., without pre-treatment) to obtain an overview of the spectral changes among açaí oil samples during oxidation. The classification analysis was realized using linear discriminant analysis (LDA) using the three first principal components (PC) of the PCA. The linear, quadratic, and Mahalanobis methods were tested. The different NIR spectral regions and pre-treatments were tested. The performance of the classification was expressed in terms of sensitivity and accuracy. The sensitivity describes the ability of the model to classify correctly samples. The accuracy is defined as the fraction of correctly classified samples with respect to the entire set.

Results and Discussion

Quality Parameters During Oxidation

The significant increase of all quality parameters (i.e., peroxide value, conjugated diene value, and *p*-anisidine value) with oxidation time whatever the treatment applied clearly indicates the formation of primary and secondary oxidation products (Choe and Min 2006) (see lower case letters in Fig. 1). Our results are comparable to the ones obtained by Silva and Rogez (2013) who is, to our knowledge, the only paper who previously studied the oxidation of açaí oil. In particular, the authors submitted açaí oil samples at 60 °C for 3, 7, and 11 days, in the presence of 400 ppm of different antioxidants, including myricetin.

Thanks to the experimental design used in our study, coupled to MANOVA statistical analysis, we can conclude that the treatment, the oxidation time, and the interaction between both factors are significant for all quality parameters (*p* value < 0.05). Only the interaction between the treatment and the oxidation time for the *p*-anisidine value is not significant (*p* value = 0.31), which can be explained by the high standard deviations (see Fig. 1c) and by the fact that it is a secondary product of oxidation. In particular, this statistical analysis allows identifying the time period that marks a sudden rise in the oxidation rate, commonly known as the induction period, which corresponds to the depletion
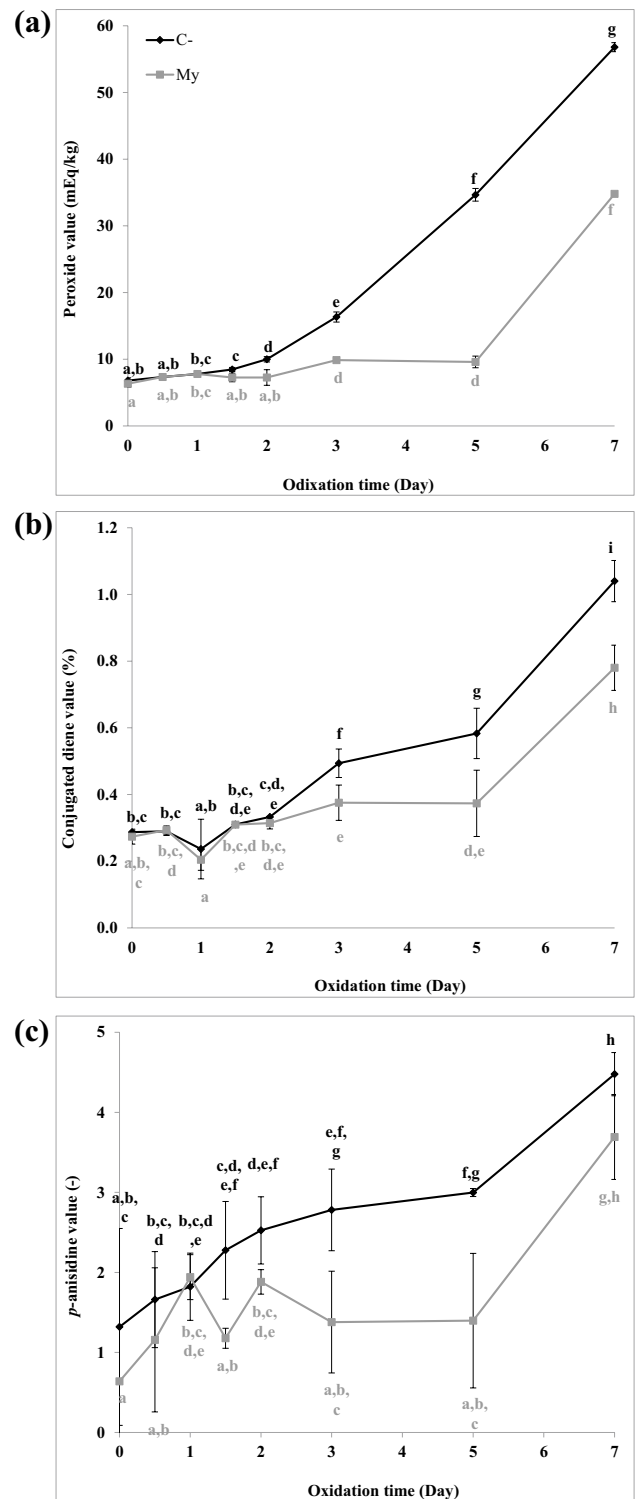

Fig. 1 Peroxide value (**a**), conjugated diene value (**b**), and *p*-anisidine value (**c**) of açaí oil without antioxidant (C-) and supplemented with 400 ppm of myricetin (My) during accelerated conditions at 60 °C for 7 days. Legend: Results are presented as the mean value ± the standard deviation (n = 3). Different lower case letters imply that the values are statistically different, using the multi-factorial analysis of variance (MANOVA) and the Fisher LSD test, with a significance level of 95% (*p* value ≤ 0.05)

of the endogeneous or exogeneous antioxidants (Kiritsakis and Shahidi 2017). The induction periods relative to treatment "C-" and "My" are approximately 1.5 to 2 days and 3 to 5 days, respectively (see Fig. 1), indicating that the sample of açaí oil without antioxidant is more sensitive to the oxidation than the one supplemented with 400 ppm of myricetin. This behavior has been observed by other authors for other vegetable oils (Wójcicki et al. 2015).

In particular, the recommended limits of the peroxide value in refined edible oil for commercialization and human consumption are defined as 10 (Codex Alimentarus 1999) and 30 mEq O_2/kg (Gotoh and Wada 2006), respectively. Açaí oil without antioxidant ("C-") exceeds these values after 2 days and 5 days of oxidation, respectively, while the addition of myricetin ("My") allows delaying this period up to 5 days and 7 days, respectively (see Fig. 1a).

Eventually, the estimation of the rate of production of the primary and secondary oxidation products per unit of time during oil oxidation also points out differences in behavior as a function of the treatment (see Table 1). According to the determination coefficients (R^2) of the linear regression, the kinetic model that best adjusted to the results of the primary oxidation products (peroxide value and conjugated diene value) of treatment samples "C-" is a first-order kinetic model ($R^2 = 0.98$ and 0.93, respectively) (see Table 1). For the secondary oxidation products (*p*-anidisine value), the best model is a zero order kinetic model ($R^2 = 0.91$). For treatment samples "My," the best models are first-order (conjugated diene value, $R^2 = 0.78$) and second-order (peroxide value, $R^2 = 0.94$; and *p*-anisidine value, $R^2 = 0.76$) kinetic models. This second-order kinetic model can be explained by the important induction period (up to 5 days) regarding to the total oxidation period (7 days).

NIR Spectral Changes During Oxidation

The NIR spectrum of açaí oil (calculated as the average of the different NIR spectra collected) shows the characteristic absorbance bands of vegetable oils with some well-defined bands (see Fig. 2) (Hourant et al. 2000). The 10,000–6500 cm^{-1} region exhibits several weak band characteristic of the second overtone of C–H stretching vibrations. More specifically, the weak bands (a) at 8600 cm^{-1} and (c) at 7100 cm^{-1} are related to the methyl group (-CH_3) while the weak bands (b) at 8200 cm^{-1} and (d) at 7000 cm^{-1} are related to the etilyl group (-CH_2-). Such bands are commonly present in oils rich in mono or polyunsaturated fatty acids. The 6100–5100 cm^{-1} region shows two main bands which are characteristics of the first overtone of C-H stretching vibrations: (e) at 5800 cm^{-1} and (f) at 5680 cm^{-1}, attributed to the presence of the linoleic and oleic acid, respectively. The 4800–4000 cm^{-1} region exhibits two bands attributed to the =CH- stretching vibration of the cis double bound (-HC=CH-) unsaturated fatty acid: (g) at 4670 cm^{-1} and (h) at 4590 cm^{-1}. This region also showed two intense absorption bands that are characteristic of the combination of C-H stretching vibration with other vibrational modes: (i) at 4340 cm^{-1} and (j) at 4266 cm^{-1}. Finally, one can observe two characteristic bands (*) due to the presence of hydroperoxides at 4800 cm^{-1} (–OH combination bands) and 6950 cm^{-1} (first overtones of O–H stretching vibrations).

The most pronounced changes of the NIR spectra of açaí oil during oxidation are observed in the spectral region from 10,000 to 6500 cm^{-1} that exhibits bands related to functional groups directly involved with oxidation of oils (see Fig. 3). One can observe an increase of the absorbance as a function of the oxidation time, whatever the treatment applied. More specifically, the NIR spectral region from 7000 to 6500 cm^{-1} is also pointed out in the literature as presenting the most significant changes due to the formation of hydroperoxides (Wójcicki et al. 2015; Costa et al. 2016).

Calibration Models by Partial Least Square Regression Method

Calibration models were developed using PLS regression method, using the full leave-one-out internal cross-validation procedure (see Table 2) and the external validation

Table 1 Evaluation of the order of the kinetic model for the three quality parameters as a function of the treatment

	PV (mEq O_2/kg)		CD (%)		pAV (-)	
	C-	My	C-	My	C-	My
k for $n=0$	7.22	3.26	0.10	0.06	**0.39**	0.29
R^2	0.93	0.67	0.90	0.76	**0.91**	0.58
k for $n=1$	**0.32**	0.20	**0.20**	**0.14**	0.15	0.15
R^2	**0.98**	0.77	**0.93**	**0.78**	0.87	0.53
k for $n=2$	− 0.015	**− 0.020**	− 0.421	− 0.353	− 0.103	**− 0.062**
R^2	0.94	**0.94**	0.87	0.69	0.42	**0.76**

k rate constant kinetic, *n* order of the kinetic model, R^2 determination coefficient, *PV* peroxide value, *CD* conjugated diene value, *pAV* p-anisidine value, *C*- açaí oil samples without antioxidant, *My* açaí oil samples supplemented with 400 ppm of myricetin

Bold numbers identify the best order of the kinetic model (k and R^2) for each quality parameter and each treatment

Fig. 2 Average NIR spectrum of açaí oil in the spectral region from 10,000 to 4000 cm⁻¹. Legend: Spectral bands a to j, and (*) are described in the text
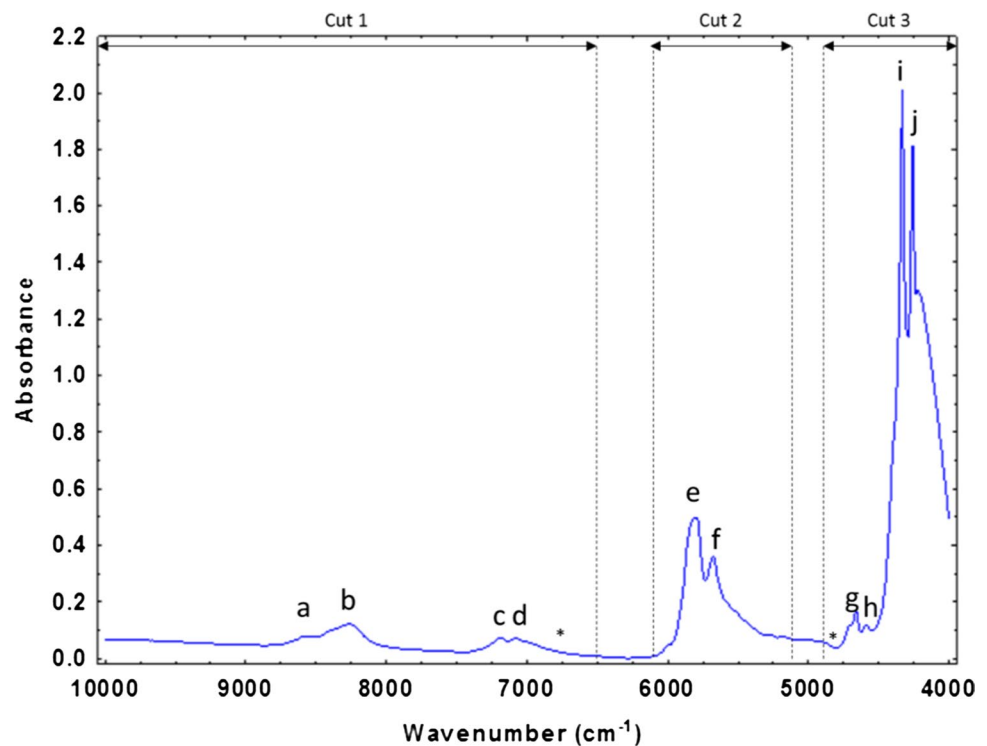
procedure (see Table 4). For this purpose, the samples were divided in two different sets: 29 samples (approximately 64% of the total number of samples) were selected as calibration set, using 2 repetitions of each experimental point, and the remaining 16 samples were employed as prediction set to validate the calibration, using the third repetition of each experimental point (see Table 3).

The different statistical parameters of the calibration models for prediction of the peroxide value are very similar whatever the NIR spectral region considered and the validation procedure used (full internal cross-validation or external validation) (see Tables 2 and 4). However, the best NIR spectral region is 10,000–6500 cm⁻¹, as presenting the highest R^2 of calibration (> 0.98), R^2 of cross-validation (0.92), R^2 of validation (0.92) and RPD (> 3.55), the smallest RMSEC (< 1.9 mEq O_2/kg), RMSECV (3.9 mEq O_2/kg), RMSEV (4.0 mEq O_2/kg), and number of PLS factors (< 7). The values obtained for these statistical parameters are coherent with previous papers that developed calibration models for prediction of peroxide value during oil oxidation (see for example Calero et al. 2018; Hong et al. 2017; Wójcicki et al. 2015; Armenta et al. 2007; Yildiz et al. 2001; Moh et al. 1999 and Cho et al. 1998). Some of these authors also studied the effect of the NIR spectral region on the quality of the calibration models and obtained similar conclusion that is our (see for example Calero et al. 2018; Moh et al. 1999; Yildiz et al. 2001; Armenta et al. 2007).

There is an important variation of the statistical parameters of the calibration model for the prediction of the conjugated diene value as a function of the NIR spectral region (see Tables 2 and 4). In particular, the two NIR spectral regions (10,000–6500 cm⁻¹ and 6100–5100 cm⁻¹) present relatively high R^2 of calibration (> 0.82), R^2 of cross-validation (> 0.58), R^2 of validation (> 0.55), and RPD (> 0.3), and small RMSEC (< 0.47%), RMSECV (< 0.74%), and RMSEV (< 0.79%). The other NIR spectral regions (whole spectra, 4800–4000, and 6100–5100 & 4800–4000 cm⁻¹) present very poor quality. One can observe that the statistical parameters are slightly better using the full internal cross-validation (Table 2) than the external validation (Table 4), mainly regarding to the RPD values (1.5 versus 0.3). The two best NIR spectral regions identified in our study and the values obtained for the different statistical parameters are coherent with previous papers who studied the prediction of the conjugated diene value by NIRS (Daoud et al. 2020; Yildiz et al. 2001).

The different statistical parameters of the calibration models for prediction of the *p*-anisidine value present a slight variation as a function of the NIR spectral region (see Tables 2 and 4). The best NIR spectral region is 10,000–6500 cm⁻¹ as presenting the highest R^2 of calibration (> 0.97), R^2 of cross-validation (0.89), R^2 of validation (0.83), and RPD (> 2.9), and the smallest RMSEC (0.04 pAV unit), RMSECV (0.07 pAV unit), RMSEV (0.10 pAV unit), and number of PLS factors (< 7). One can observe that the statistical parameters are slightly better using the external validation (Table 4) than the full internal
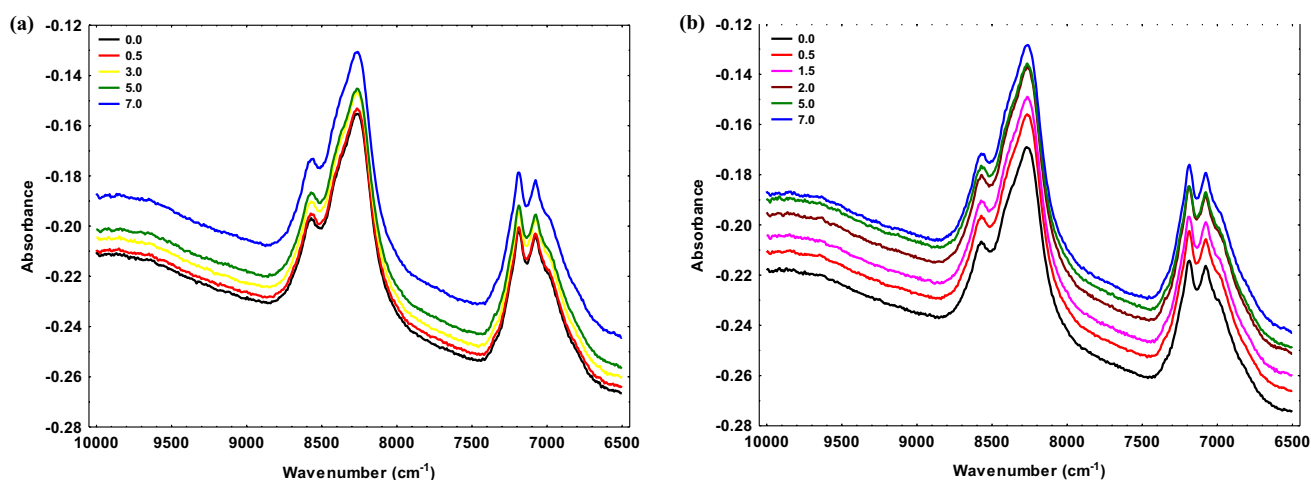
Fig. 3 Variation of the absorbance of the NIR spectra in the spectral region from 10,000 to 6500 cm^{-1} as a function of the oxidation time for açaí oil without antioxidant (**a**) and supplemented with 400 ppm of myricetin (**b**)

cross-validation (Table 2), mainly regarding to the RPD values (12.73 versus 2.9). The best NIR spectral region identified in our paper and the values obtained for the different statistical parameters are coherent with previous papers who studied the prediction of the *p*-anisidine value during oil oxidation (Calero et al. 2018; Yildiz et al. 2001).

In conclusion, one of the best NIR spectral region for the development of calibration models for prediction by PLS method for the three quality parameters is 10,000–6500 cm^{-1}, which is coherent with previous papers. Moreover, as commonly observed in the literature, the best statistical parameters of the calibration models are obtained for the prediction of the peroxide value and *p*-anisidine value (Yildiz et al. 2001). The models are characterized by R^2 of calibration > 0.97, R^2 of cross-validation > 0.89, R^2 of validation > 0.83, and RPD > 2.9, which indicates good performance for the prediction of new independent samples (Wójcicki et al. 2015).

Principal Component Analysis of NIR spectra

The spectral changes occurring during oil oxidation are evaluated using PCA on the raw NIR spectra (i.e., without pre-treatments), as presenting the best visualization for discrimination (see Fig. 4). The PC1 and PC2 explain 85 and 14%, respectively, of the total variability of the data occurring during oxidation. Two main conclusions may be highlighted. First, PCA exhibits a logical organization of the points according to the oxidation time, highlighted by the pathway from day 0 to day 7. Such behavior was previously reported by Wójcicki et al. (2015), who used the combination of MIRS and NIRS to study the oxidation of olive, sunflower, and rapeseed oils during accelerated oxidative degradation. Second, it is interesting to observe that,

although with a slight overlap, the PCA shows the formation of two sample clusters. Most of colored points, i.e., points from day 0 to day 1.5, are located in the left part of the PCA. Such points are relative to açaí oil samples presenting peroxide value below the limit of 10 mEq O$_2$/kg (see Fig. 1a). On the other hand, points relative to açaí oil unfit for commercialization are located in the right part of the PCA. A similar discrimination of oil by PCA was previously reported by Costa et al. (2016), who used NIRS to classify soybean oil samples according to expiration date (correlated to the peroxide value). PCA turns out a fast, practical, and visual tool for the decision to preserve or throw away açaí oil samples at industrial scale.

Classification Analysis

The classification parameters of the LDA are presented for the different NIR spectral regions, without pre-treatment and with the pre-treatment that gives the best results of sensitivity and accuracy (see Table 5). The worst performance parameters of classification as a function of the oxidation time are obtained using the NIR spectral data without pre-treatment whatever the NIR spectral region considered (accuracy < 89%). The classification analysis using the quality parameters obtained by reference analysis presents highest sensitivity and accuracy (91.1%). Eventually, the use of pre-treatments of the NIR spectral data allows increasing the classification parameters. The use of the NIR spectral regions 6100–5100 cm^{-1} (with normalize and second derivative, or SNV and first derivative) and 6100–5100 and 4800–4000 cm^{-1} (with smoothing) also presents an accuracy of 91.1%. The use of the NIR spectral region 10,000–6500 cm^{-1} with the pre-treatments MSC and first derivative, or SNV and First derivative, allows an accuracy of 95.6% (see Table 5). In particular, the sensitivities are

Table 2 Cross-validation statistics of the PLS calibration models for prediction of the three quality parameters as a function of the NIR spectral region

Quality parameter	NIR spectral region	Calibration		Cross-validation		RPD	PLS factors
		R^2	RMSEC	R^2	RMSECV		
PV	Whole spectra	0.978	2.036	0.804	6.262	2.12	9
(mEq O_2/kg)	6100–5100 & 4800–4000 cm^{-1}	0.969	2.454	0.711	7.599	1.82	9
	6100–5100 cm^{-1}	0.949	3.112	0.735	7.283	1.90	7
	4800–4000 cm^{-1}	0.960	2.752	0.403	10.923	1.27	9
	10,000–6500 cm^{-1}	**0.981**	**1.902**	**0.924**	**3.898**	**3.55**	**6**
CD	Whole spectra	0.259	0.960	0.186	1.030	1.08	2
(%)	6100–5100 & 4800–4000 cm^{-1}	0.272	0.952	0.181	1.033	1.08	2
	6100–5100 cm^{-1}	**0.913**	**0.329**	**0.578**	**0.741**	**1.51**	**7**
	4800–4000 cm^{-1}	0.239	0.973	0.178	1.035	1.08	1
	10,000–6500 cm^{-1}	**0.819**	**0.475**	**0.683**	**0.643**	**1.74**	**5**
pAV	Whole spectra	0.968	0.040	0.623	0.139	1.60	9
(-)	6100–5100 & 4800–4000 cm^{-1}	0.941	0.054	0.486	0.162	1.37	8
	6100–5100 cm^{-1}	0.910	0.066	0.657	0.132	1.67	6
	4800–4000 cm^{-1}	0.954	0.047	0.232	0.198	1.12	9
	10,000–6500 cm^{-1}	**0.967**	**0.040**	**0.886**	**0.076**	**2.90**	**6**

R^2 determination coefficient, *RMSEC* root mean of error of calibration, *RMSECV* root mean of error of cross-calibration, *RPD* ratio of prediction to deviation, *PV* peroxide value, *CD* conjugated diene value, *pAV* p-anisidine value

Bold lines identify the best NIR spectral region(s) for each quality parameter

100% for all oxidation times except for "day 0" and "day 1" where the sensitivities are 83.3%, signifying that only one sample is not classified correctly. It is interesting to mention that Costa et al. (2016) also identified that the best LDA classification performance (96%) of 50 samples of soybean oil according to expiration date was obtained for the NIR spectral region from 10,000 to 6500 cm^{-1} and with the first derivative as pre-treatment.

Conclusions

In our opinion, the important finding of our study is the demonstrated potential of the use of NIRS and chemometrics for the evaluation of quality parameters of açaí oil with and without supplementation during thermal oxidation. In particular, thanks to the experimental design used, our paper points out that the supplementation of açaí oil with myricetin allows delaying the induction period. Our study also concludes that NIRS coupled to PLS calibration models and LDA classification models allows predicting correctly quality parameters and classifying correctly açaí oil samples as a function of the oxidation time, respectively. Eventually, our work shows that açaí oil samples can be easily discriminated as safe or unfit for commercialization using PCA. Such findings could be useful for laboratories and industries leading with açaí oil, mainly in the Amazonian Region.

Table 3 Composition of the calibration and validation datasets for prediction of the three quality parameters using NIRS

Quality parameter	Calibration set				Validation set			
	N	Average	deviation	Range	n	Average	deviation	Range
PV (mEq O_2/kg)	29	15.44	14.89	6.40–57.20	16	14.74	14.37	5.80–56.01
CD (%)	29	0.40	0.22	0.17–1.06	16	0.41	0.24	0.14–1.09
pAV (-)	29	2.12	1.08	0.06–4.79	16	2.09	1.21	0.06–4.30

N number of samples, *PV* peroxide value, *CD* conjugated diene value, *pAV* p-anisidine value

Table 4 External validation statistics of the PLS calibration models for prediction of the three quality parameters as a function of the NIR spectral region

Quality parameter	NIR spectral region	Calibration		Validation		RPD	PLS factors
		R^2	RMSEC	R^2	RMSEV		
PV	Whole spectra	0.997	0.76	0.698	7.68	1.87	10
(mEq O_2/kg)	6100–5100 & 4800–4000 cm^{-1}	0.965	2.58	0.554	9.34	1.54	8
	6100–5100 cm^{-1}	0.972	2.31	0.331	11.43	1.26	6
	4800–4000 cm^{-1}	0.935	3.51	0.402	10.82	1.33	7
	10,000–6500 cm^{-1}	**0.996**	**0.82**	**0.917**	**4.03**	**3.57**	**7**
CD	Whole spectra	0.819	0.46	0.253	1.01	0.23	6
(%)	6100–5100 & 4800–4000 cm^{-1}	0.455	0.78	0.053	1.42	0.17	2
	6100–5100 cm^{-1}	**0.972**	**0.18**	**0.549**	**0.79**	**0.30**	**7**
	4800–4000 cm^{-1}	0.436	0.81	0.11	1.11	0.21	2
	10,000–6500 cm^{-1}	**0.951**	**0.24**	**0.704**	**0.64**	**0.37**	**6**
pAV	Whole spectra	0.996	0.01	0.474	0.17	7.29	10
(-)	6100–5100 & 4800–4000 cm^{-1}	0.995	0.02	0.520	0.16	7.66	10
	6100–5100 cm^{-1}	0.926	0.06	0.089	0.22	5.55	6
	4800–4000 cm^{-1}	0.991	0.02	0.460	0.17	7.20	9
	10,000–6500 cm^{-1}	**0.995**	**0.02**	**0.829**	**0.10**	**12.73**	**7**

R^2 determination coefficient, *RMSEC* root mean of error of calibration, *RMSEV* root mean of error of validation, *RPD* ratio of prediction to deviation, *PV* peroxide value, *CD* conjugated diene value, *pAV* p-anisidine value

Bold lines identify the best NIR spectral region(s) for each quality parameter

Declarations

Ethics Approval Not applicable.

Consent to Participate Not applicable.

Conflict of Interest B.V.C. Rodrigues declares that she has no conflict of interest. D.R. Pompeu declares that he has no conflict of interest. C.A.N.P Herman declares that she has no conflict of interest.

References

Armenta S, Garrigues S, Guardia M (2007) Determination of edible oil parameters by near infrared spectrometry. Anal Chim Acta 596:330–337. https://doi.org/10.1016/j.aca.2007.06.028

Barriuso B, Astiasarán I, Ansoren D (2013) A review of analytical methods measuring lipid oxidation status in foods: a challenging task. Eur Food Res Technol 236(1):1–15. https://doi.org/10.1007/s00217-012-1866-9

Batista CCR, Oliveira MS, Araújo ME, Rodrigues AMC, Botelho JRS, Filho APSS, Machado NT, Junior RNC (2016) Supercritical CO_2 extraction of açaí (*Euterpe oleracea*) berry oil: global yield, fatty acid, allelopathic activities, and determination of phenolic and anthocyanins total compounds in the residual pulp. J Supercrit Fluids 107:364–369. https://doi.org/10.1016/j.supflu.2015.10.006

Calero AM, Muñoz E, Pérez-Marin D, Riccioli C, Pérez L, Garrido-Varo A (2018) Evolution of frying oil quality using fourier transform near-infrared (FT-NIR) spectroscopy. Appl Spectrosc 72(7):1001–1013. https://doi.org/10.1177/0003702818764125

Canha N, Felizardo P, Menezes JC, Correia MJN (2012) Multivariate near infrared spectroscopy models for predicting the oxidative stability of biodiesel: effect of antioxidants addition. Fuel 97:352–357. https://doi.org/10.1016/j.fuel.2012.02.017

Cho S-Y, Kim J-Y, Rhee C (1998) Determination of rancidity of soybean oil by near infrared spectroscopy. J near Infrared Spectrosc 6:A349–A354. https://doi.org/10.1255/jnirs.222

Choe E, Min DB (2006) Mechanisms and factors for edible oil oxidation. Compr Rev Food Sci Food Saf 5(4):169–186. https://doi.org/10.1111/j.1541-4337.2006.00009.x
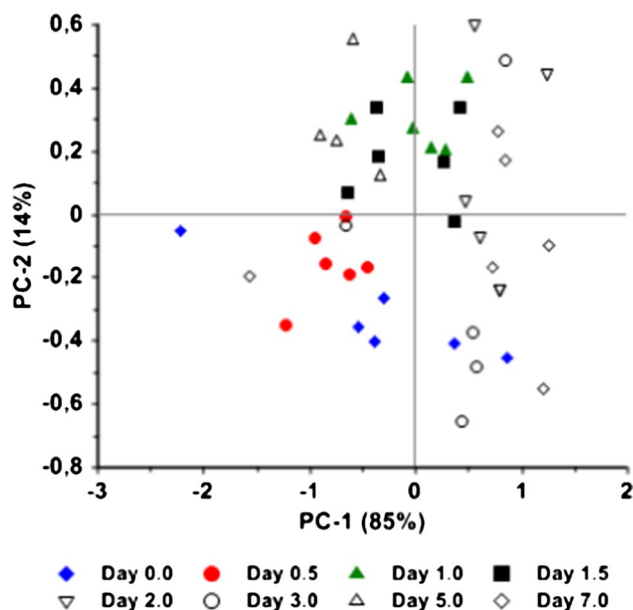
Fig. 4 PC1 versus PC2 score plot of the PCA of raw NIR spectra for all açaí oil samples

Table 5 Classification parameters of sensitivity and accuracy by applying the linear discriminant analysis to the NIR spectral data and to the quality parameters data

NIR Spectral region	Pre-treatment applied	Discrimination performance of oxidation time of açaí oil samples (day)								
		Sensitivity								Accuracy
		0.0	0.5	1.0	1.5	2.0	3.0	5.0	7.0	
Whole spectra	- (raw spectra)	83.3%	100%	100%	83.3%	100%	60.0%	100%	33.3%	82.2%
10,000–6500 cm^{-1}		100%	100%	83.3%	83.3%	100%	40.0%	100%	66.7%	84.4%
6100–5100 cm^{-1}		83.3%	100%	100%	66.7%	66.7%	80.0%	100%	33.3%	77.8%
4800–4000 cm^{-1}		50.0%	100%	83.3%	66.7%	83.3%	60.0%	100%	66.7%	75.6%
6100–5100 & 4800–4000 cm^{-1}		83.3%	100%	100%	100%	100%	60.0%	100%	66.7%	88.9%
Whole spectra	MSC	100%	83.3%	83.3%	83.3%	100%	100%	100%	66.7%	88.9%
10,000–6500 cm^{-1}	**MSC and First derivative**	**83.3%**	**100%**	**83.3%**	**100%**	**100%**	**100%**	**100%**	**100%**	**95.6%**
	SNV and First derivative	**83.3%**	**100%**	**83.3%**	**100%**	**100%**	**100%**	**100%**	**100%**	**95.6%**
6100–5100 cm^{-1}	Normalize and Second derivative	83.3%	100%	83.3%	83.3%	100%	100%	100%	83.3%	91.1%
	SNV and First derivative	100%	100%	66.7%	83.3%	100%	100%	100%	83.3%	91.1%
4800–4000 cm^{-1}	Normalize and First derivative	100%	100%	100%	66.7%	100%	80.0%	100%	50.0%	86.7%
6100–5100 & 4800–4000 cm^{-1}	Smoothing	100%	100%	100%	100%	100%	60.0%	100%	66.7%	91.1%
Quality parameters obtained by reference analysis		83.3%	83.3%	83.3%	100%	100%	100%	75.0%	100%	91.1%

Bold lines identify the best NIR spectral region and pre-treatment(s)

Choe E, Min DB (2009) Mechanisms of antioxidants in the oxidation of foods. Compr Rev Food Sci Food Saf 8(4):345–358. https://doi.org/10.1111/j.1541-4337.2009.00085.x

Codex Alimentarus (1999) Codex for edible fats and oils not covered by individual s. CODEX STAN 19–1981, Rev. 2–1999. Rome, Italy: Codex Alimentarius

Costa GB, Fernandes DDS, Gomes AA, Almeida VE, Veras G (2016) Using near infrared spectroscopy to classify soybean oil according to expiration date. Food Chem 196:539–543. https://doi.org/10.1016/j.foodchem.2015.09.076

Cozzolino D, Murray I, Chree A, Scaife JR (2005) Multivariate determination of free fatty acid and moisture in fish oils by partial least-squares regression and near-infrared spectroscopy. LWT 38(8):821–828. https://doi.org/10.1016/j.lwt.2004.10.007

Daoud S, Waschatko G, Bou-Maroun E, Cayot P (2020) Fast, direct and in situ monitoring of lipid oxidation in an oil-in-water emulsion by near infrared spectroscopy. Anal Methods 12:3098–3105. https://doi.org/10.1039/D0AY00583E

Darnet S, Serra JL, Rodrigues AMC, Silva LHM (2011) A high-performance liquid chromatography method to measure tocopherols in assai pulp (Euterpe oleracea). Food Res Int 44:2107–2111. https://doi.org/10.1016/j.foodres.2010.12.039

Favacho HAS, Oliveira BR, Santos KC, Medeiro BJL, Sousa PJC, Perazzo FF, Carvalho JCT (2011) Anti-inflammatory and antinociceptive activities of Euterpe oleracea oil. Rev Bras Farmacogn 21(1):105–114. https://doi.org/10.1590/S0102-695X2011005000007

Filho ALM, Pereira MRR (2012) Antimicrobial activity of açaí and pupunha oils on the development of Pseudomonas aeruginosa and Staphylococcus aureus. Biosci J 28(4):598–603

Gotoh N, Wada S (2006) The importance of peroxide value in assessing food quality and food safety. JAOCS 83(5):473–474. https://doi.org/10.1007/s11746-006-1229-4

Hong S-Y, Rho S-J, Lee A-Y, Park H, Cui J, Park J, Hong S-J, Kim Y-R, Kim G (2017) Rancidity estimation of perilla seed oil by using near-infrared spectroscopy and multivariate analysis techniques. J Spectrosc 1082612:10. https://doi.org/10.1155/2017/1082612

Hourant P, Baeten V, Morales MT, Meurens M, Aparicio R (2000) Oil and fat classification by selected bands of near-infrared spectroscopy. Appl Spectrosc 54:1168–1174. https://doi.org/10.1366/0003702001950733

Kiritsakis A, Shahidi F (2017) Olives and olive oil as functional foods: bioactivity, chemistry and processing, First Edition. Online ISBN:9781119135340. https://doi.org/10.1002/9781119135340

Laguerre M, Lecomte J, Villeneuve P (2007) Evaluation of the ability of antioxidants to counteract lipid oxidation: existing methods, new trends and challenges. Prog Lipid Res 46:244–282. https://doi.org/10.1016/j.plipres.2007.05.002

Lubrano C, Robin JR, Khaiat A (1994) Fatty acid, sterol and tocopherol composition of oil from the fruit mesocarp of six palm species in French Guiana. Oléagineux

Moh MH, Man YBC, van de Voort FR, Abdullah WJW (1999) Determination of peroxide value in thermally oxidized crude palm oil by near infrared spectroscopy. JAOCS 76(1):19–23

Monge-Fuentes V, Muehlmann LA, Longo JP, Silva JR, Fascineli ML, de Souza P, Faria F, Degterev I, Rodriguez A, Carneiro FP, Lucci CM, Escobar P, Amorim RF, Azevedo RB (2017) Photodynamic therapy mediated by açai oil (Euterpe oleracea Martius) in nanoemulsion: a potential treatment for melanoma. J Photochem Photobiol b: Biology 166:301–310. https://doi.org/10.1016/j.jphotobiol.2016.12.002

Muresan V, Danthine S, Muresan AE, Racolta E, Blecker C, Muste S, Socaciu C, Baeten V (2016) In situ analysis of lipid oxidation in oilseed-based food products using near-infrared spectroscopy and chemometrics: the sunflower kernel paste (Tahini) Example. Talanta 155:336–346. https://doi.org/10.1016/j.talanta.2016.04.019

Pacheco-Palencia LA, Talcott SM, Talcott ST (2008) Chemical composition, antioxidant properties, and thermal stability of a phytochemical enriched oil from açai (Euterpe oleracea Mart.). J Agric Food Chem 56:4631–4636. https://doi.org/10.1021/jf800161u

Plotkin MJ, Balick M (1984) Medicinal uses of South American palms. J Ethnopharmacol 10:157–179

Sánchez JAC, Moreda W, Garcia JM (2013) Rapid determination of olive oil oxidative stability and its major quality parameters using Vis/NIR transmittance spectroscopy. J Agric Food Chem 61:8056–8062. https://doi.org/10.1021/jf4021575

Schauss AG (2010) Açai (Euterpe oleracea Mart.): a macro and nutrient rich palm fruit from the Amazon rain forest with demonstrated bioactivities in vitro and in vivo. In: Watson DR, Preedy VR (eds) Bioactive foods promotion health. Academic Press, Oxford, pp 479–490

Silva JJM, Rogez H (2013) Evaluation of oxidative stability of crude açai (*Euterpe oleracea*) oil in the presence of pure phenolic compounds or Amazonian plant extracts. Quím Nova 36(3):400–406. https://doi.org/10.1590/S0100-40422013000300009

Souza MO, Silva LS, Magalhães CLB, Figueiredo BB, Costa DC, Silva ME, Pedrosa ML (2012) The hypocholesterolemic activity of açai (Euterpe oleracea Mart.) is mediated by the enhanced expression of ATP-binding cassette, subfamily G transporters 5 and 8 low-density lipoprotein receptor genes in rat. Nutr Res 32:976–984. https://doi.org/10.1016/j.nutres.2012.10.001

Wójcicki K, Khmelinskii I, Sikorski M, Sikorska E (2015) Near and mid infrared spectroscopy and multivariate data analysis in studies of oxidation of edible oils. Food Chem 187:416–423. https://doi.org/10.1016/j.foodchem.2015.04.046

Yildiz G, Wehling RL, Cuppet SL (2001) Method for determining oxidation of vegetable oils by near-infrared spectroscopy. JAOCS 78:495–502. https://doi.org/10.1007/s11746-001-0292-1